Measurement of sound absorption with a dual-plane array of microphone by an optimization approach

Samuel Dupont, Manuel Melon, Alain Berry

MEASUREMENT OF SOUND ABSORPTION WITH A DUAL-PLANE ARRAY OF MICROPHONE BY AN OPTIMIZATION APPROACH

Samuel Dupont [1] **Manuel Melon** [1] **Alain Berry**[2]

[1] Laboratoire d'Acoustique de l'Université du Mans (LAUM) UMR CNRS 6613, Le Mans Université, Le Mans, France
[2] Groupe d'Acoustique de l'Université de Sherbrooke (GAUS), Université de Sherbrooke, Sherbrooke, Canada
Manuel.Melon@univ-lemans.fr, Alain.Berry@usherbrooke.ca

ABSTRACT

This paper proposes the improvement of a recently published method for measuring the sound absorption and the surface impedance of an acoustic material using a double planar array of microphones. It uses an optimization process on the surface impedance, which matches the measured sound pressure field to a theoretical model. The previous model calculated the complete solution of a point source over an infinite layer of material, but had the disadvantage of having a high computational cost. The model proposed in this paper is based on the classical image source approximation. The results shows an excellent accuracy in high frequency, where the approximation is good. However, the approximate model is not as accurate as the previous one in low frequency. The gain in computing time with the approximate model is significant: a factor of 30 is observed. Experimental validations are performed in a semi-anechoic room with a layer of melamine foam using a 3D positioning system to move a single 1/2" microphone. The measured surface impedance is compared to the measurements obtained with an impedance tube. Overall, both methods give good results between 200 Hz and 6000 Hz.

1. INTRODUCTION

Standard sound absorption methods such as the impedance tube work very well but have the disadvantage of measuring only a small sample at normal incidence [1]. The second standard method uses a reverberation chamber to measure an average absorption coefficient in the diffuse field. It is well known for its non-physical results and severe non-repeatability, especially at low frequencies [2–6]. Conventional methods for measuring sound absorption *in situ* generally use very few microphones. These methods have inherited some of the above mentioned defects, while introducing new ones [7]. On the other hand, with the rise of low-cost MEMS technology, it is now possible to create robust microphone arrays at an affordable cost. This has led to a renewed interest in microphone antennas for measuring sound absorption. The ultimate goal is to be able to measure absorption *in situ*, while overcoming the problems of standardized and conventional methods. Recent publications on the subject have mostly focused on holographic approaches [8–10], or the approximation of local plane waves [11]. This presentation shows the improvement of a recently presented method [12]. It is based o n an optimization process which uses a simplified point source propagation model on an impedance plane. This method is studied here for a double layer plane microphone array under various incidences. Simulations of the measurement method and experimental results are presented. A brief discussion of the advantages and disadvantages of this new implementation is presented.

2. THEORETICAL BACKGROUND

2.1 Problem definition

The measurement configuration consists of a double square planar array of $K = 50$ (2×25) microphones with a side length a, a spacing c placed at a distance h above the acoustic material whose normalized surface impedance Z_s is to be characterized. The sound field is generated by a point source and is reflected by the infinite planar surface of the acoustic material. A scheme is presented in Fig. 1.

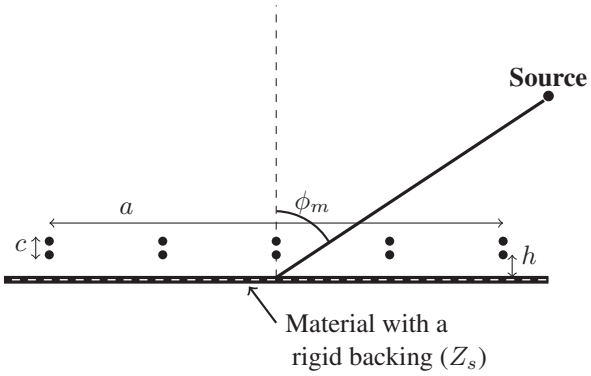

Figure 1: A point source and a planar microphone array above a material of normalized surface impedance Z_s.

2.2 Optimisation

The optimization process minimizes using the Matlab *fminsearch* function the cost function $\mathcal{J}$:

$$\mathcal{J} = \text{argmin}(\|\mathbf{p}(\mathbf{r}_l, Z_s, A) - \mathbf{p}^{\mathbf{meas}}\|_2^2) \qquad (1)$$

where A is the amplitude (modulus and phase) of the source, $\mathbf{p} \in \mathbb{C}^{K\text{x}1}$ is the vector containing the sound

pressures associated with the transfer functions between a point source located in $\mathbf{r}_l(x_l, y_l, z_l)$ and the sound pressures at K antenna microphone positions for the selected model. The vector $\mathbf{p^{meas}} \in \mathbb{C}^{K\text{x}1}$ is the measurement associated with the $\mathbf{p}$ model. Z_{init} is the initial value of Z_s at each frequency in the optimization process. The process is carried out in the frequency domain, starting with the high frequencies and continuing towards the low frequencies using the previously found solution as initial values. The initial value is here estimated by a simulation impedance Z_s from the Johnson-Champoux-Allard (JCA) model [13] model, but others, like Miki model [14] can be used. $\mathbf{r}_{init}$ is the position of the source relative to the center of the antenna estimated on the measurement setup. A_{init} is calculated with $A_{init} = \|\mathbf{p^{meas}}\|_2 r_{init}$.

The process minimizes the error between the model and the measured acoustics by the microphone array, it aims to calculate the 'best' Z_s corresponding to the configuration. Such an approach has been detailed in [12] with the use of a point source above an infinite layer of impedance model, a second simplified model is studied in this paper.
The configuration of the subsequent models with the different geometrical quantities is shown in Fig. 2.

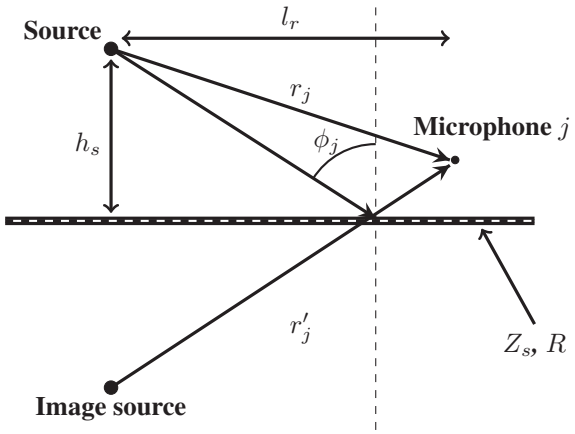

Figure 2: Diagram of a source point and a microphone above a plane with impedance Z_s.

The time convention $e^{j\omega t}$ is used in this paper.

2.3 Point source above an infinite layer of impedance model

Full details of the method can be found in [12], but are briefly presented here for the sake of completeness. The first model evaluates p at each microphone position, considering the solution of a point source above an infinite layer of impedance Z_s [15], as follows:

$$p(\mathbf{r}_l, Z_s, A) = A\left(\frac{e^{-ikr_j}}{r_j} + \frac{e^{-ikr'_j}}{r'_j} - 2\frac{k}{Z_s}I_1\right), \quad (2)$$

with k the wave number and I_1 defined by:

$$I_1 = \int_0^\infty \frac{e^{-ikr'_j[(1-\xi^2-2i\xi\sin\phi_j)^{1/2}-i\xi/Z_s]}}{(1-\xi^2-2i\xi\sin\phi_j)^{1/2}}d\xi. \quad (3)$$

The evaluation of I_1 is the most expensive part of the optimization process because it evaluates the integral at each iteration. This model will be referred to as 'COSI inf' in the following.

2.4 Approximated image source model

In order to reduce the calculation cost, the classical image source method [16, 17] is used. The p model is therefore evaluated at each microphone as follows:

$$p(\phi_j, \omega) = A\left(\frac{e^{-ikr_j}}{r_{ml}} + R(\phi_j, \omega)\frac{e^{-ikr'_j}}{r'_j}\right), \quad (4)$$

with the reflection coefficient $R(\phi_j, \omega)$ related to the normalized surface impedance Z_s per:

$$Z_s = \frac{1+R(\phi_j,\omega)}{1-R(\phi_j,\omega)}\frac{\sqrt{l_r^2+h_s^2}}{h_s}\frac{ik\sqrt{l_r^2+h_s^2}}{1+ik\sqrt{l_r^2+h_s^2}} \quad (5)$$

thus given by:

$$R(\phi_j, \omega) = \frac{Z_s - \frac{\sqrt{l_r^2+h_s^2}}{h_s}\frac{ik\sqrt{l_r^2+h_s^2}}{1+ik\sqrt{l_r^2+h_s^2}}}{Z_s + \frac{\sqrt{l_r^2+h_s^2}}{h_s}\frac{ik\sqrt{l_r^2+h_s^2}}{1+ik\sqrt{l_r^2+h_s^2}}}. \quad (6)$$

This model will be referred to as 'COSI approx' in the following.

Once Z_s is obtained, the sound absorption α can be calculated assuming an incident plane wave:

$$\alpha = 1 - \left|\frac{Z_s\cos\phi_j - 1}{Z_s\cos\phi_j + 1}\right|^2. \quad (7)$$

3. SIMULATIONS

Several simulations are then presented in order to compare the advantages and disadvantages of the two methods. The first simulations show the results without noise, followed by results with the introduction of a white noise signal and finally with the presence of reflections. The point source is placed at $r_l = 1.5$ m and three elevations are tested: $\psi_m = 0°$, $30°$ and $60°$. The microphone array has a side length a of 0.14 m, a spacing c of 0.015 m and a distance from the material surface $h = 0.01$ m. The 'exact' normalized surface impedance of the material with a rigid support is calculated using the JCA model [13] whose input parameters are given in the Table 1. The formulation given in Eq (2) is used to calculate the sound pressure field radiated by the point source above the impedance plane Z_s assumed to be infinite.
It is noted that since the same model is used for both the generation and optimization of 'COSI inf', this could result in a bias in the results. However, this approach is sufficient to make a general comment on the method before the experimental validation.

3.1 Results without measurement noise

These first simulations in the absence of measurement noise presented in Fig. 3 aim at showing the limits of the two models by considering a perfect case. Both methods are able to estimate accurately the plane wave absorption α and the normalized surface impedance Z_s especially at high frequency. However, at low frequencies, 'COSI inf' shows much better performance than 'COSI approx'. For the latter, we can explain that below $ka \approx 1$ ($\approx$ 380 Hz), especially near the material, the approximate model is not accurate enough to represent the physics of the problem because the interaction between the material and the source is rather complex and modeled by Eq. 3. This means that there are significant differences between the model and the measurement, resulting in the failure of the optimization process at low frequencies. As for the 'COSI inf' model, the results are good up to a frequency of 100 Hz ($ka \approx 0.26$). Although the inverse crime may be an explanation, it is more likely that the interaction between the source and the material in the model is sufficiently well defined to allow the optimization process to converge. Below 100 Hz, the wavelength is too large relative to the size of the array, causing the optimization process to fail due to the lack of information in the observations. The use of the 'COSI approx' model compared to the 'COSI inf' model is therefore recommended for frequencies above $ka = 1$ because there is no interest in using the full model, considering that the cost of the calculation is reduced by a factor of 30.

3.2 Results with a Signal to Noise Ratio (SNR) of 30 dB

The results of the simulations in the presence of measurement noise (SNR of 30 dB) are presented in Fig. 4. The results at high frequency are as good as without measurement noise, which is normal because the influence of white noise is negligible compared to the amount of information contained in the high-frequency observations (especially for the phase). In these simulations, both models are accurate down to 400 Hz, where the noise starts to significantly disturb the measurement data. In this case, the noise deteriorates the measurement so that no information prior to $ka = 1$ can be obtained, the use of the 'COSI inf' model below $ka = 1$ is then worthless.

3.3 Results with acoustics reflections

The results of simulations in the presence of point source reflected in a room are presented in Fig. 5. The room consists of infinite walls that are modeled by first-order image sources only. The walls and ceiling are covered with 60 cm thick rock wool (Miki model [14], static airflow resistivity $\sigma = 1500$ N.s.m^{-4}). The melamine foam that covers rigid floors is the one that must be characterized. This simulation is therefore far from physical, but the intention here is only to show that there is an influence of reflections. It therefore does not show the effect of nearby reflections, such as the first reflections of the measuring devices or the edge effect of the material. It will only affect low to mid frequencies, because the absorption of the walls is close to 1 in high frequency. The infinite walls are located at x = 3.2 m and x = -5.8 m, y = -2.6 m and y = 3.5 m, z = 4 m.
When the source is at normal and low incidence, the result does not differ from that obtained without any measurement noise as in Fig. 3. However, when the incidence is high (Fig. 5.c and Fig. 5.f), the results start to deteriorate because the two models fail to converge below 300 Hz. The fact that the reflections only affect the measurement at high incidence in low frequency is explained by the fact that the value of the particle velocity u_z is very low. In addition, a projection on the normal to the material is performed at oblique incidence, due to the fact the velocity field is propagating in the direction of the source and not in the direction of the normal to the material. The quantity u_z on the surface of the material to be characterized thus becomes very sensitive to the surrounding disturbances.
In a real case, it is to be expected that the reflections will have a greater influence than the present result due to edge effects, measurements apparatus reflections and higher-order reflections from the room.

4. MEASUREMENTS RESULTS

The measurements were carried out in the semi-anechoic room of LAUM to characterize a sample of melamine foam of 1.8 m $\times$ 1.2 m. A three-dimensional (3D) positioning system was used to move a 1/2" B&K type 4192 microphone. The microphone is positioned successively at the different desired positions (about 1 minute per microphone position).The results are then assembled to create a single antenna measurement. This kind of set up avoid calibration issues related to array of microphones which is a critical problem at low frequency. The results of the measurement with the melamine foam are compared to the result of the impedance tube method, whose JCA parameters have been characterized (see table 1). The measurement configuration is presented in Fig. 6. The results at normal incidence are presented in Fig. 7.a and Fig. 7.c. They corroborate with what has already been observed in simulation. In high frequency, both models give an accurate result, while the 'COSI approx' does not converge below $ka \approx 1$ and the 'COSI inf' does not converge below $ka \approx 0.26$ and seems to be affected by reflection as small oscillations are present. The results at $\phi_m = 30°$ are shown in Fig. 7.b and Fig. 7.d. In high frequency, both models give an accurate result. The two methods do not converge below $ka \approx 1$ ($\approx$ 380 Hz), which probably indicates that reflections disturb the measurement because both methods are affected while measurement noise is the same than at normal source incidence.

4.1 Comments on the measurement and simulation configuration

The parameter c was chosen to be equal to 1.5 cm however further simulations showed that best results in low frequency were obtained with $c = 3.5$ cm which corresponds to the step size step size of the microphone grid.

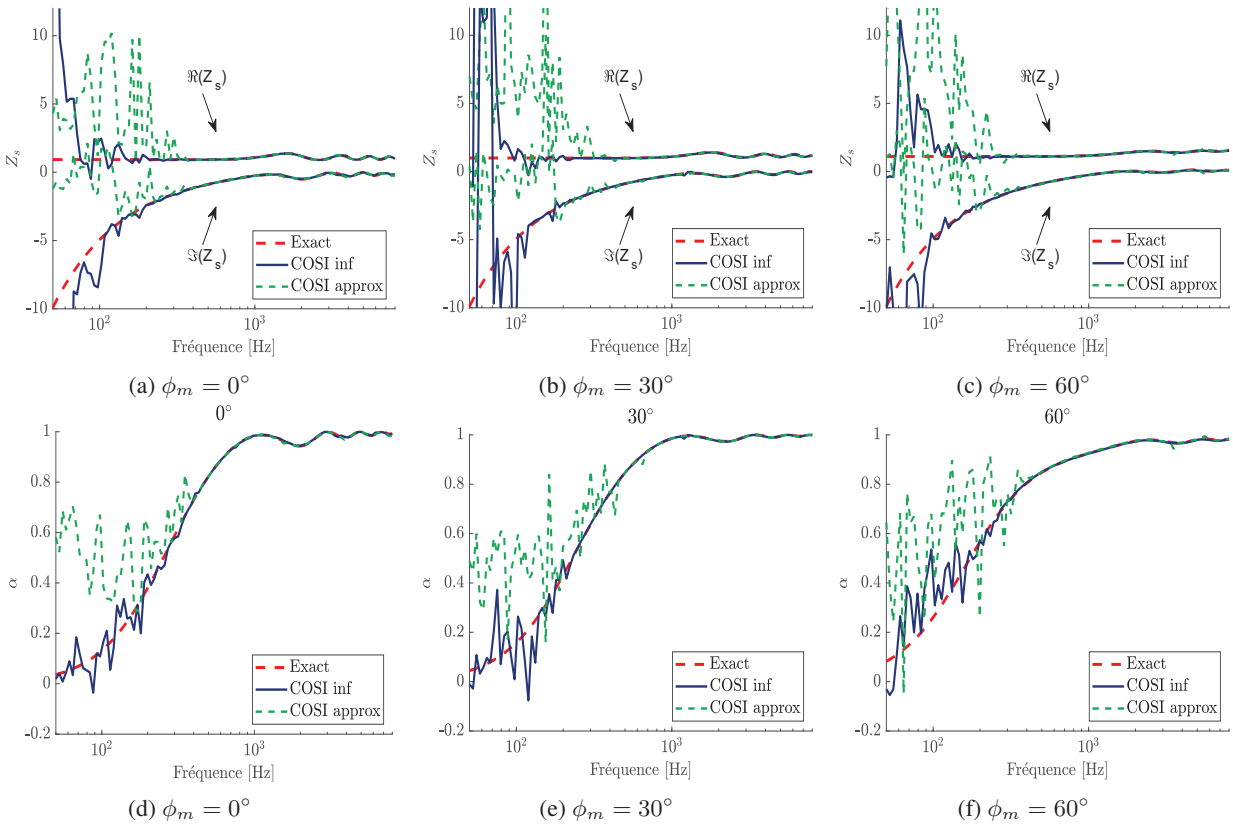

(a) $\phi_m = 0°$ (b) $\phi_m = 30°$ (c) $\phi_m = 60°$

(d) $\phi_m = 0°$ (e) $\phi_m = 30°$ (f) $\phi_m = 60°$

Figure 3: Estimated absorption and normalized surface impedance for a source at 0°, 30° and 55° without noise. Figures (a) to (c): $\Re(Z_s)$ and $\Im(Z_s)$ and Figures (d) to (f): α.

5. CONCLUSION

This paper presents the comparison of two models used in an optimization process to determine the normalized surface impedance Z_s and the sound absorption α of the acoustic material with a double planar array of microphones. The first model has already been presented in a paper while the second model used here is the classical approximation of the image source model. The second model does not outperform the result of the first one, however a computational time gain factor of 30 is observed. The second model shows inaccurate results below $ka = 1$, which is normal because it does not correctly model the interaction between the acoustic material and the microphones when the source is close. It is therefore suggested to use a combination of the two models: model 2, 'COSI approx' above $ka = 1$ and model 1, 'COSI inf' below $ka = 1$. Different types of perturbations have also been numerically investigated, showing that both models are robust to white noise, but give poor results in low frequencies when reflections are introduced in the measurements. Taking into account reflections due to edge effects, measurement apparatus and room reflections when performing a free-field characterization of an acoustic material remains a challenge for the future. Although these results do not show it, both models show good robustness to reflections in high frequencies. Further developments regarding the inclusion of reflections in the approximate model are currently under investigation.

A. APPENDIX

σ	11500	[N.s.m^{-4}] Static air flow resistivity
h_a	0.08	[m] Height of the material
ϕ	0.998	Porosity
Λ	124	[μm] Viscous length
Λ'	183	[μm] Thermal length
α_∞	1.005	Tortuosity

Table 1: Melamine foam JCA parameters

B. REFERENCES

[1] H. Koruk, "An assessment of the performance of impedance tube method," *Noise Control Engineering Journal*, vol. 62, no. 4, pp. 264–274, 2014.

[2] V. L. Chrisler, "Dependence of sound absorption upon the area and distribution of the absorbent material," *Journal of Research of the National Bureau of Standards*, vol. 13, no. 2, pp. 169–187, 1934.

[3] R. E. Halliwell, "Inter-laboratory variability of sound absorption measurement," *The Journal of the Acoustical Society of America*, vol. 73, no. 3, pp. 880–886, 1983.

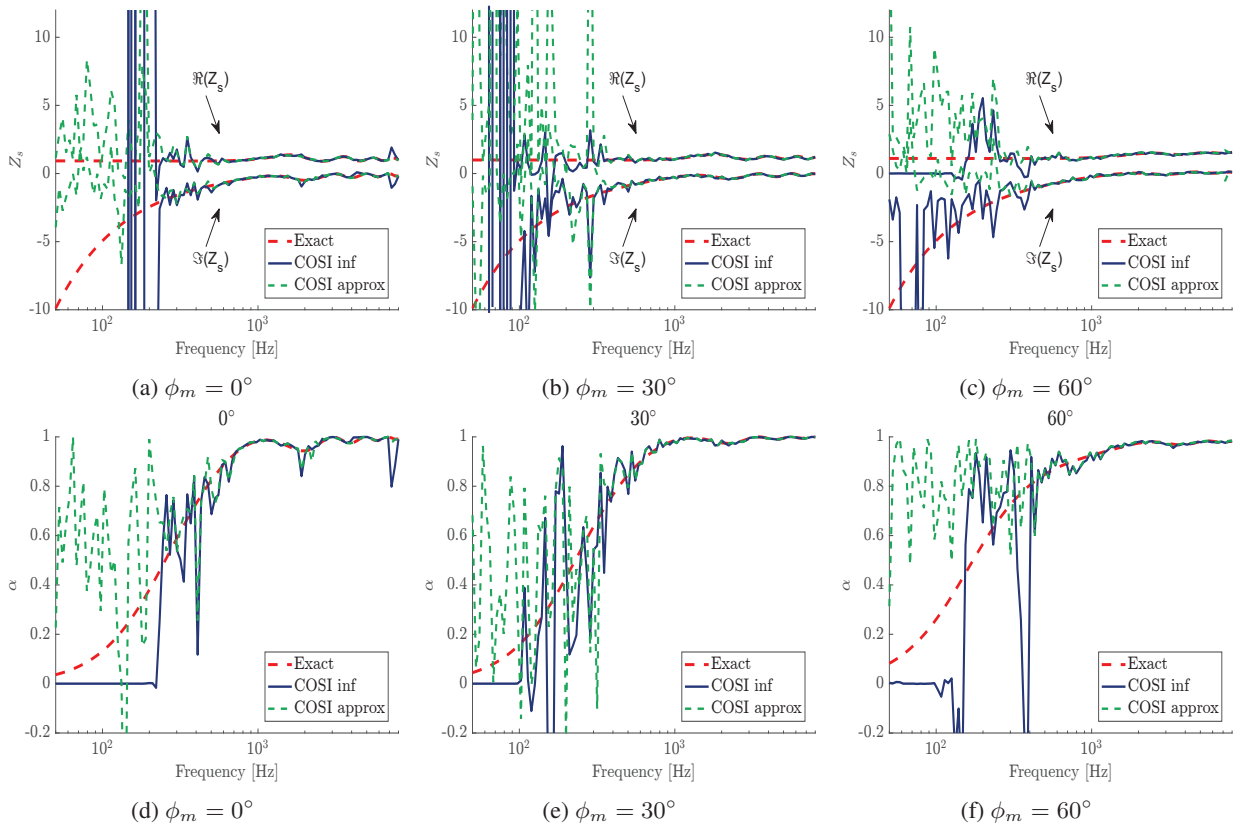

(a) $\phi_m = 0°$ (b) $\phi_m = 30°$ (c) $\phi_m = 60°$

(d) $\phi_m = 0°$ (e) $\phi_m = 30°$ (f) $\phi_m = 60°$

Figure 4: Estimated absorption and normalized surface impedance for a source at 0°, 30° and 55° with a 30 dB SNR. Figures (a) to (c): $\Re(Z_s)$ and $\Im(Z_s)$ and Figures (d) to (f): α.

[4] E. Toyoda, S. Sakamoto, and H. Tachibana, "Effects of room shape and diffusing treatment on the measurement of sound absorption coefficient in a reverberation room," *Acoustical science and technology*, vol. 25, no. 4, pp. 255–266, 2004.

[5] M. Vercammen, "Improving the accuracy of sound absorption measurement according to ISO 354," in *Proceedings of the International Symposium on Room Acoustics, Melbourne, Australia*, 2010.

[6] A. Nash, "On the reproducibility of measuring random incidence sound absorption," *The Journal of the Acoustical Society of America*, vol. 130, no. 4, pp. 2354–2354, 2011.

[7] E. Brandão, A. Lenzi, and S. Paul, "A review of the in situ impedance and sound absorption measurement techniques," *Acta Acustica united with Acustica*, vol. 101, no. 3, pp. 443–463, 2015.

[8] A. Richard, E. Fernandez-Grande, J. Brunskog, and C.-H. Jeong, "Estimation of surface impedance at oblique incidence based on sparse array processing," *The Journal of the Acoustical Society of America*, vol. 141, no. 6, pp. 4115–4125, 2017.

[9] A. Richard and E. Fernandez-Grande, "Comparison of two microphone array geometries for surface impedance estimation," *The Journal of the Acoustical Society of America*, vol. 146, no. 1, pp. 501–504, 2019.

[10] M. Nolan, S. A. Verburg, J. Brunskog, and E. Fernandez-Grande, "Experimental characterization of the sound field in a reverberation room," *The Journal of the Acoustical Society of America*, vol. 145, no. 4, pp. 2237–2246, 2019.

[11] M. Ottink, J. Brunskog, C.-H. Jeong, E. Fernandez-Grande, P. Trojgaard, and E. Tiana-Roig, "In situ measurements of the oblique incidence sound absorption coefficient for finite sized absorbers," *The Journal of the Acoustical Society of America*, vol. 139, no. 1, pp. 41–52, 2016.

[12] S. Dupont, M. Melon, and A. Berry, "Characterization of acoustic material at oblique incidence using a spherical microphone array," *The Journal of the Acoustical Society of America*, vol. 147, no. 5, pp. 3613–3625, 2020.

[13] J. F. Allard and N. Atalla, *Propagation of Sound in Porous Media: Modelling Sound Absorbing Materials*. Wiley, 2. ed ed., 2009. OCLC: 699014950.

[14] Y. Miki, "Acoustical properties of porous materials-Modifications of Delany-Bazley models," *Journal of the Acoustical Society of Japan (E)*, vol. 11, no. 1, pp. 19–24, 1990.

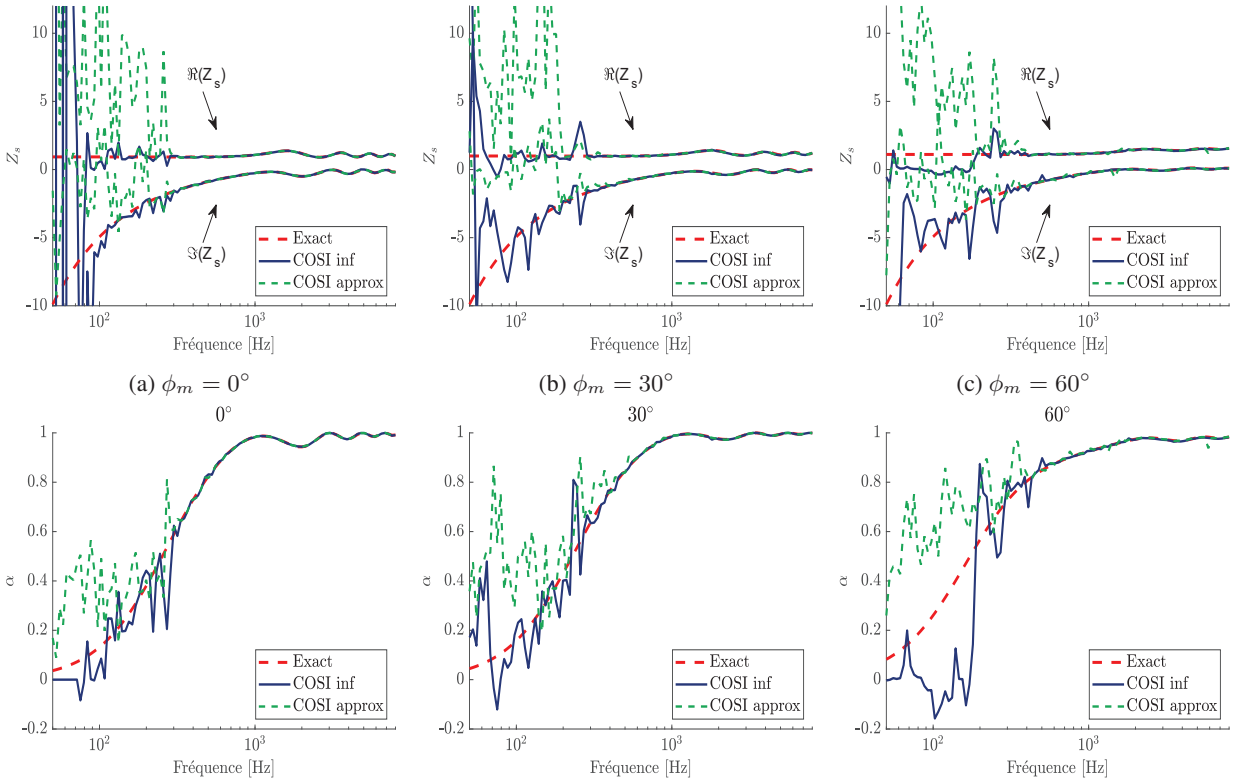

(a) $\phi_m = 0°$ (b) $\phi_m = 30°$ (c) $\phi_m = 60°$

(d) $\phi_m = 0°$ (e) $\phi_m = 30°$ (f) $\phi_m = 60°$

Figure 5: Estimated absorption and normalized surface impedance for a source at 0°, 30° and 55° with reflections. Figures (a) to (c): $\Re(Z_s)$ and $\Im(Z_s)$ and Figures (d) to (f): α.

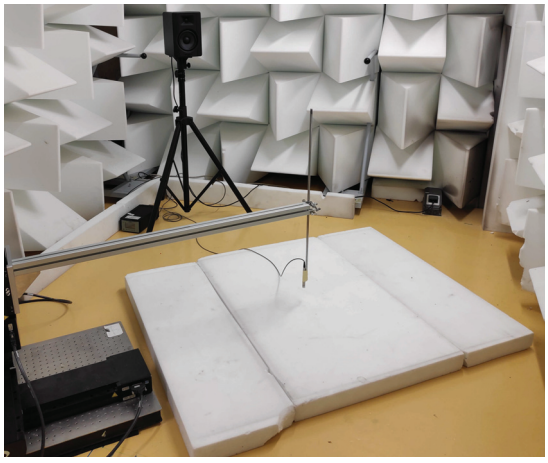

Figure 6: Measurement set-up with a source.

[15] S. I. Nobile, Matthew A. et Hayek, "Acoustic propagation over an impedance plane," *The Journal of the Acoustical Society of America*, vol. 78, no. 4, pp. 1325–1336, 1985.

[16] J. Daniel, B. Alvarez, and F. Jacobsen, "In-situ measurements of the complex acoustic impedance of porous materials," in *INTER-NOISE and NOISE-CON Congress and Conference Proceedings, Istanbul, Turquie*, vol. 2007, pp. 3873–3882, Institute of Noise Control Engineering, 2007.

[17] E. Brandão, E. Tijs, A. Lenzi, and H.-E. de Bree, "A Comparison of Three Methods to Calculate the Surface Impedance and Absorption Coefficient from Measurements Under Free Field or in situ Conditions," *Acta Acustica united with Acustica*, vol. 97, no. 6, pp. 1025–1033, 2011.

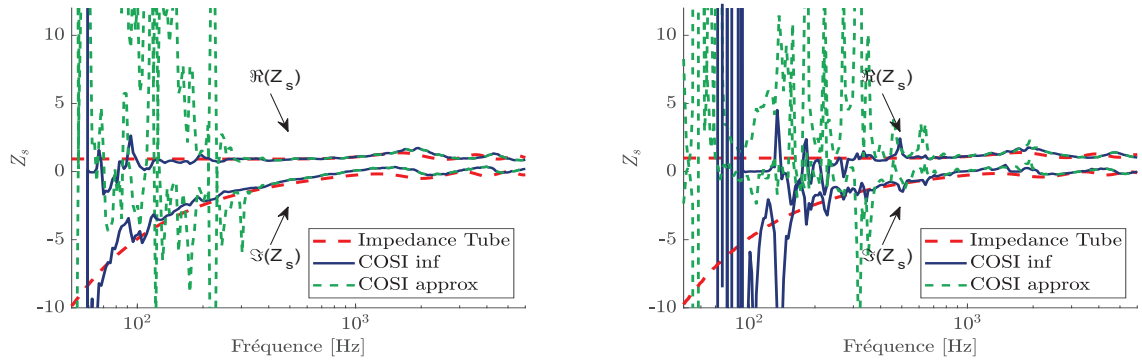

(a) $\phi_m = 0°$ (b) $\phi_m = 30°$

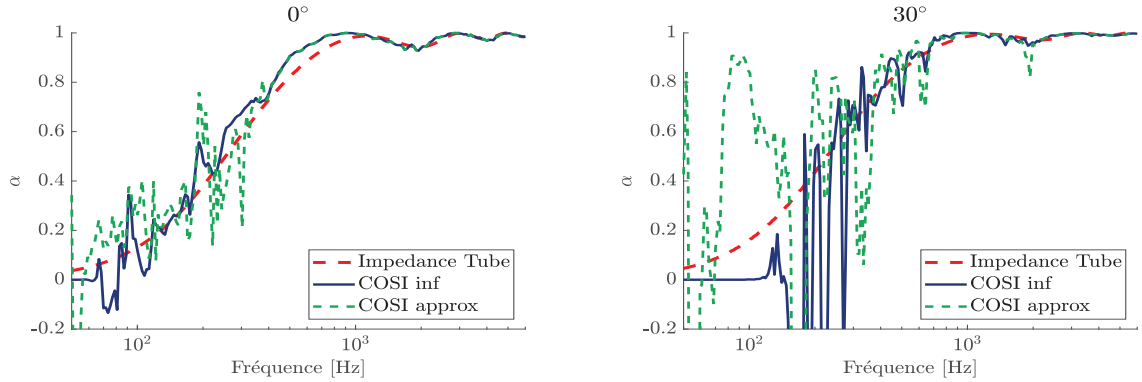

(c) $\phi_m = 0°$ (d) $\phi_m = 30°$

Figure 7: Estimated absorption and normalized surface impedance of the melamine foam for a source at 0°, 30° in the semi-anechoic room. (a) to (c): $\Re(Z_s)$ and $\Im(Z_s)$ and (d) to (f): α.